Molecular Medicine

Xanthine Oxidoreductase Function Contributes to Normal Wound Healing

Michael C Madigan,[1,2] Ryan M McEnaney,[1,2] Ankur J Shukla,[1,2] Guiying Hong,[1,2] Eric E Kelley,[3] Margaret M Tarpey,[1,3] Mark Gladwin,[4] Brian S Zuckerbraun,[1,2] and Edith Tzeng[1,2]

[1]Surgery Services, Department of Veterans Affairs Medical Center, Pittsburgh, Pennsylvania, United States of America; Departments of [2]Surgery, [3]Anesthesia, and [4]Medicine, University of Pittsburgh, Pittsburgh, Pennsylvania, United States of America

Chronic, nonhealing wounds result in patient morbidity and disability. Reactive oxygen species (ROS) and nitric oxide (NO) are both required for normal wound repair, and derangements of these result in impaired healing. Xanthine oxidoreductase (XOR) has the unique capacity to produce both ROS and NO. We hypothesize that XOR contributes to normal wound healing. Cutaneous wounds were created in C57Bl6 mice. XOR was inhibited with dietary tungsten or allopurinol. Topical hydrogen peroxide (H_2O_2, 0.15%) or allopurinol (30 μg) was applied to wounds every other day. Wounds were monitored until closure or collected at d 5 to assess XOR expression and activity, cell proliferation and histology. The effects of XOR, nitrite, H_2O_2 and allopurinol on keratinocyte cell (KC) and endothelial cell (EC) behavior were assessed. We identified XOR expression and activity in the skin and wound edges as well as granulation tissue. Cultured human KCs also expressed XOR. Tungsten significantly inhibited XOR activity and impaired healing with reduced ROS production with reduced angiogenesis and KC proliferation. The expression and activity of other tungsten-sensitive enzymes were minimal in the wound tissues. Oral allopurinol did not reduce XOR activity or alter wound healing but topical allopurinol significantly reduced XOR activity and delayed healing. Topical H_2O_2 restored wound healing in tungsten-fed mice. *In vitro*, nitrite and H_2O_2 both stimulated KC and EC proliferation and EC migration. These studies demonstrate for the first time that XOR is abundant in wounds and participates in normal wound healing through effects on ROS production.

Online address: http://www.molmed.org
doi: 10.2119/molmed.2014.00191

INTRODUCTION

Chronic, nonhealing wounds arise from diverse etiologies such as diabetes, venous stasis and pressure. Wounds occur in 12–25% of diabetic patients and contribute to a high incidence of limb loss and death (1). Despite improvements in glycemic control, antibiotics, and wound care adjuvants, nonhealing wounds continue to present a formidable problem. The underlying molecular mechanisms of impaired wound healing are poorly understood despite extensive knowledge of the normal wound repair process. Efficient wound repair involves many cytokines, chemokines and growth factors that regulate the inflammatory and regenerative phases of wound healing (2). Unfortunately, novel therapies targeting these factors, such as topical platelet-derived growth factor, have had limited success (3).

Inflammation is a necessary response to tissue injury, leading to the production of nitric oxide (NO) and reactive oxygen species (ROS) and reactive nitrogen species (RNS) that mediate oxidative stress (4). Recent evidence demonstrates that physiologic oxidative stress is essential for normal wound healing (5,6). Redox signaling has been reported to play an important role in antibiosis, hemostasis, inflammation, re-epithelialization, angiogenesis and growth factor modulation (7,8). However, an overabundance of inflammatory by-products has deleterious effects on the wound (4). For example, ROS contributed to the failure of wound healing in a rodent ischemic flap model (9) and high doses of topical hydrogen peroxide (H_2O_2) delayed wound repair by reducing collagen deposition and angiogenesis (10). Achieving the ideal balance of ROS/RNS in damaged tissues may determine wound healing efficiency.

Wound repair also depends on NO. NO synthesis in wounds occurs through the arginine-NO synthase (NOS) pathway (11) and modulates inflammation, chemotaxis, antibacterial defenses, collagen production and angiogenesis

Address correspondence to *Edith Tzeng, Chief of Vascular Surgery, VA Pittsburgh Healthcare System, Professor of Surgery, Department of Surgery, University of Pittsburgh, A1010 PUH, 200 Lothrop Street, Pittsburgh, PA 15213. Phone: 412-802-3025; Fax: 412-291-1669; E-mail: tzenge@upmc.edu.*
Submitted September 23, 2014; Accepted for publication April 14, 2015; Published Online (www.molmed.org) April 14, 2015.

(12–14). NO deficiency has been implicated in the delayed wound healing in diabetic rodent models (15,16), where NOS was downregulated. In addition, arginase I uses L-arginine to produce polyamines and proline, both essential for collagen synthesis and cell proliferation, and is induced and competes for the NOS substrate (16–18). Inducible NOS (iNOS) or endothelial NOS (eNOS) deficiency both delayed wound closure in normal mice, whereas restoration of NOS activity in these mice improved healing (19,20), supporting an essential role of NO in wound repair.

Xanthine oxidoreductase (XOR) is a homodimeric enzyme that metabolizes xanthine and generates ROS. It is also a potent nitrite reductase, converting nitrite back to NO (21,22). This pathway is especially efficient in hypoxia, a condition that reduces NOS-dependent NO production. We and others have reported that nitrite can serve as a source of NO through XOR in models of vascular injury and pulmonary hypertension (23,24). XOR has been detected in skin, where it is involved in ROS production in response to lipopolysaccharide (LPS) (25) and ultraviolet irradiation (26). Thus, we hypothesize that XOR participates in normal wound healing through ROS/RNS and NO production. We used a murine excisional wound-healing model and manipulated XOR activity (27,28) to examine its role in normal wound repair.

MATERIALS AND METHODS

Excisional Wound Healing Model

All procedures conformed to the *Guide for the Care and Use of Laboratory Animals* (29) and the policies of the Institutional Animal Use and Care Committee of the University of Pittsburgh (protocol #1104675A). Male C57BL/6 mice (8–12 wks old; The Jackson Laboratory, Bar Harbor, ME, USA) were anesthetized with Nembutal (70 mg/kg, Abbott Labs, Chicago, IL, USA) and isoflurane. After shaving, a 1.5 × 1.5–cm excisional wound was created on the back of each mouse and then covered with bio-occlusive dressings (Systagenix, Quincy, MA, USA). Wound area was measured by acetate tracings every other day until wound closure. The areas were calculated using MetaMorph® (Version 7.7.5.0; Molecular Devices, Inc., Sunnyvale, CA, USA). Wounds were also collected at earlier time points for protein and immunohistochemical analyses.

Dietary and Topical Wound Treatments

Tungsten-enriched diet (#960350; MP Biomedicals, Irvine, CA, USA) was started 2 wks before wounding to optimize molybdenum replacement in XOR and maintained thereafter. Allopurinol (100 mg/kg/day; Sigma-Aldrich, St. Louis, MO, USA) in drinking water, sodium nitrite (300 mg/L in deionized water; Sigma-Aldrich) or nitrite-free diet (Harlan Teklad amino acid diet, TD 99366; Harlan, Indianapolis, IN, USA) was initiated 1 wk before wounding and continued.

Topical H_2O_2 was applied to the wound as a 0.15% H_2O_2 solution (Thermo Fisher Scientific Inc., Waltham, MA, USA) in normal saline, and the wound was covered. Topical allopurinol (30 μg/wound) was similarly applied to each wound. Treatment was initiated immediately after wounding and continued every other day.

Western Blot Analysis

Wound samples were collected and divided into the granulation tissue and the wound edge. Skin adjacent to the wound was also collected. Samples were homogenized in lysis buffer (Cell Signaling Technology, Danvers, MA, USA) and quantified using a Pierce® BCA Protein assay (Thermo Fisher Scientific). Western blot analysis for XOR (rabbit monoclonal, 1:5,000; ab109235; Abcam, Cambridge, MA, USA), iNOS (rabbit polyclonal, 1:200; ab15323; Abcam) or arginase I (mouse monoclonal, 1:2,000; BD Biosciences, San Jose, CA, USA) was performed using horseradish peroxidase–linked goat anti-rabbit or anti-mouse secondary antibody (1:10,000; Thermo Fisher Scientific). The membranes were developed by using Super-Signal® West Pico Chemiluminescent #34080 (Thermo Fisher Scientific).

Wound Immunohistochemistry

Wounds were collected on d 7 or at wound closure and fixed in 2% paraformaldehyde, cryoprotected in 30% sucrose, embedded in OCT (Tissue Tek®; Sakura Finetek, Torrance, CA, USA) and sectioned (7 μm). Sections were treated with rabbit polyclonal anti-XOR (1:100; Santa Cruz Biotechnology, Santa Cruz, CA, USA), rabbit polyclonal anti-collagen I (1:200; Abcam), monoclonal anti-Ki67 (1:200; Abcam) or rat monoclonal anti-CD31 (1:50; BD Biosciences) antibody followed by goat anti-rabbit 488 or goat anti-rat Cy5 at 1:1,000 (Invitrogen [Thermo Fisher Scientific]). Nuclei were counterstained with Hoechst 33325 (2 μg/mL, Sigma-Aldrich). Images were collected using the Fluoview® FV1000 confocal microscope (Olympus, Center Valley, PA, USA).

Wound Angiogenesis

Wound sections were stained with CD31, and two confocal images of the wound granulation tissue were obtained for each section. Wound angiogenesis was calculated as the number of CD31-stained lumens with ImageJ (version 1.45s; National Institutes of Health, Bethesda, MD, USA) and as the percent area of CD31 staining using MetaMorph®.

XOR and Aldehyde Oxidase Activity

XOR activity was quantified as described (23) via HPLC with electrochemical detection. Briefly, endogenous uric acid (UA) was removed by using a Sephadex G-25 column (GE Healthcare, Waukesha, WI, USA). Samples were then treated with oxonic acid (2 mmol/L) to inhibit uricase. XOR activity was quantified by UA production after addition of xanthine (75 μmol/L). Total XDH activity was assessed by exposure to NAD^+ (0.5 mmol/L) and pyruvic acid (5 mmol/L). The specificity for XOR activity was verified by allopurinol inhibitable UA formation. Aldehyde oxidase (AO) ac-

tivity was measured by incubating tissue homogenates with the AO substrate 4-(dimethylamino)cinnamaldehyde (DMAC) (25 μmol/L in potassium phosphate [KPi], pH 7.8, and at 25°C) and monitored for a decrease in absorbance at 398 nm.

Wound ROS/RNS Measurement

Total ROS/RNS was quantified by using the OxiSelect™ In Vitro ROS/RNS Assay Kit (Cell Biolabs, Inc., San Diego, CA, USA) per instructions. Homogenized wound tissues (50 μg) were assayed for ROS/RNS by the conversion of dichlorodihydrofluorescein to 2′,7′-dichlorodihydrofluorescein diacetate.

In Vitro Studies in Keratinocyte Cells and Endothelial Cells

Human epidermal keratinocyte cells (KCs) (PCS-200-011; ATCC, Manassas, VA, USA) were cultured in Dermal Cell Basal Media (PCS-200-030, ATCC) plus Keratinocyte Growth Kit (PCS-200-040, ATCC). KCs were differentiated with 1.2 mmol/L of calcium. Whole cell lysates were used for Western blot analysis for XOR (1:100; Santa Cruz). For immunocytochemistry, KCs were cultured on glass slides, fixed with 2% paraformaldehyde, blocked in 2% BSA in PBS and then incubated with rabbit polyclonal anti-XOR (1:100; Santa Cruz) and mouse monoclonal anti-K10 (1:100; Abcam) followed by secondary goat anti-rabbit or anti-mouse antibody (1:1,000). Nuclei were counterstained with Hoechst 33325 (2 μg/mL) (Sigma-Aldrich). Images were acquired on the Fluoview® FV1000 confocal microscope (Olympus).

Human dermal microvascular endothelial cells (ECs) (VEC Technologies; Rensselaer, NY, USA) were cultured as described (30) and low passage was used. Briefly, cells were grown in a 1:1 mix of MCDB131 (VEC Technologies) and Dulbecco modified Eagle medium (DMEM) with 5% fetal bovine serum (FBS). In proliferation assays, ECs were cultured in DMEM with 1% FBS overnight. Proliferation was measured by using ^{3}H-thymidine as described (31) in 1% FBS medium with nitrite, H_2O_2, catalase or allopurinol (Sigma-Aldrich). Migration was measured using the scratch assay at 6 h (32) and quantified with ImageJ. For *in vitro* angiogenesis, ECs were cultured on Matrigel™ (BD Biosciences) as described (30) with and without nitrite, allopurinol, H_2O_2 or catalase. Tube formation was examined at 6 h, quantifying boxes and number of long tubes (>110 pixels in length) as a marker of healthy tubes.

Statistical Analysis

Data are presented as mean ± standard error of the mean (SEM). Statistical analysis was performed with a Student *t* test or analysis of variance by using the SigmaStat 11.0 software (Systat Software Inc., San Jose, CA), and significance was determined at $P < 0.05$. All pairwise multiple comparisons were performed by using the Holm-Sidak method.

RESULTS

XOR, iNOS and Arginase I Expression in Wound Tissue

C57BL/6 mouse skin had easily detectable XOR expression by Western blot (Figure 1A). XOR expression was not altered by allopurinol, tungsten and nitrite diets (data not shown). The wound edge had less XOR expression, whereas the granulation tissue had the lowest. In contrast, iNOS expression was minimal in the skin but was upregulated in the wound edge and granulation tissue (Figure 1A). Arginase I had a similar expression pattern to iNOS (Figure 1A). Immunostaining of wounds at d 7 and after healing at d 14 revealed that the epidermal KCs expressed high levels of XOR (Figure 1B). Much less XOR was detected in the dermis or subcutaneous tissues. XOR expression was most pronounced in the thick, proliferating layer of KCs surrounding the healing wound as well as in the thinner layer of KCs in normal skin. At 2 d after wounding (Figure 1C), the upregulation of XOR expression in the wound edge was evident compared with the surrounding skin. In addition, there were cells in the peri-wound dermis and subcutaneous tissues that stained for XOR and are consistent with neutrophils by the appearance of the nuclear morphology. This finding indicates that XOR is highly expressed in the wound throughout the healing process and early inflammatory infiltrates also express XOR. Cultured KCs also expressed XOR by immunostaining and Western blot (Figures 1D, E). Differentiation of the KCs with calcium, as indicated by the expression of keratin-10, did not affect XOR expression.

Tungsten-Inhibited XOR Activity and Delayed Wound Healing in C57BL/6 Mice

Tungsten substitutes for the molybdenum (Mb) in XOR, inhibiting it irreversibly. Tungsten diet significantly inhibited skin XOR activity compared with mice fed allopurinol (18.5 ± 15.2 versus 147.6 ± 4.8 μU/mg protein, $P < 0.001$) or a chow diet (165.3 ± 10.7 μU/mg protein, $P < 0.001$) (Figure 2A). XOR activity was similar between allopurinol and control mice. XOR activity at the wound edge was moderately reduced in allopurinol-treated versus control mice (100.9 ± 15.5 versus 178.7 ± 12.1 μU/mg protein, $P < 0.001$) but tungsten-treated mice had near complete inhibition of XOR activity (6.6 ± 4.1 μU/mg protein, $P < 0.001$ versus control or allopurinol). Both allopurinol and tungsten-treated mice (35.3 ± 14.4 and 4.6 ± 2.9 μU/mg protein, respectively) had significantly less XOR activity in granulation tissue than control mice (107.6 ± 8.3 μU/mg protein, $P < 0.01$ versus tungsten or allopurinol). Wound healing was significantly delayed in mice receiving the tungsten-enriched diet versus mice on chow (Figure 2B; 21.2 ± 0.7 versus 16.4 ± 0.2 d, $P < 0.001$). Dietary allopurinol did not delay wound healing (Figure 2B).

Because oral allopurinol was much less effective in blocking XOR activity in wounds and skin than tungsten, we examined the effect of locally applied allopurinol on wound healing in mice. Topical allopurinol significantly impaired wound healing at nearly all time points

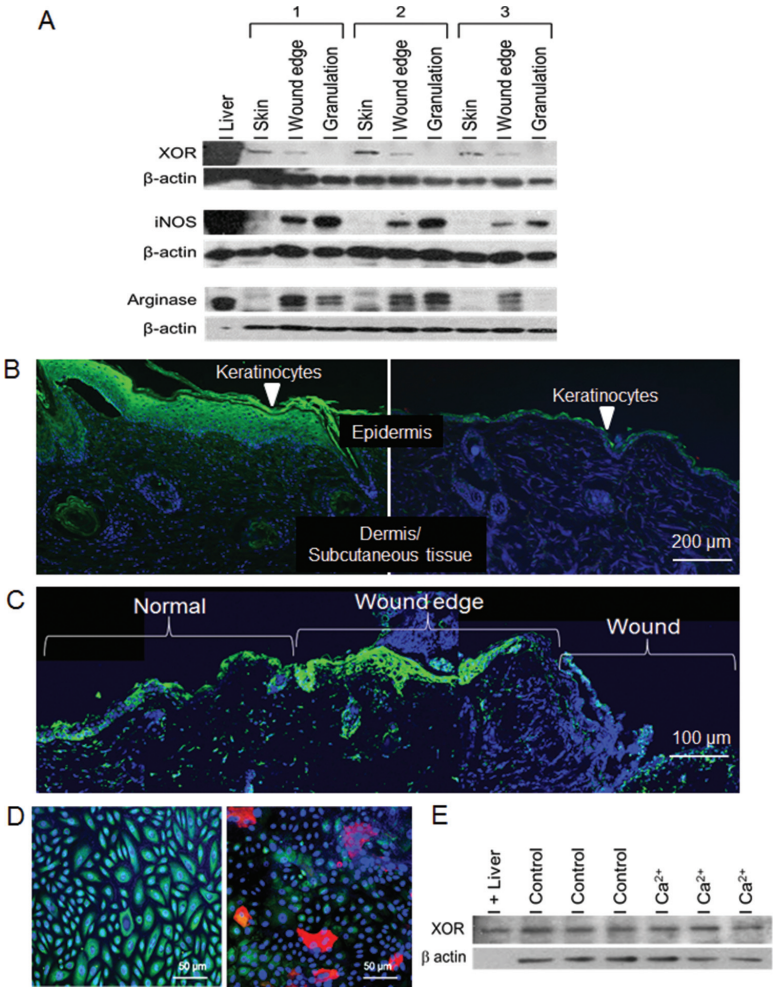

Figure 1. Examination of XOR expression in wounds and keratinocytes. (A) Western blot analysis for XOR, iNOS and arginase I expression in mouse skin, wound edge and granulation tissue is shown. Wound samples at d 7 from three separate animals are represented. β-Actin was used as a loading control. (B) XOR expression in healing wounds at d 14 (left) and normal skin (right) was examined by immunostaining (green = XOR, blue = nuclei, red = collagen; magnification of 100×). The area of the healing wound that is shown is the healed area adjacent to the wound bed. (C) XOR expression in early wounds (d 2) is demonstrated on a panoramic view showing normal skin, wound edge and the wound (green = XOR, blue = nuclei). (D) Immunostaining of cultured undifferentiated (left) and differentiated (right) human keratinocytes (200× magnification; green = XOR, blue = nuclei, red = keratin; representative photomicrographs, n = 3/group). (D) Western blot analysis for XOR expression in cultured human keratinocytes. Treatment with Ca^{2+} differentiated the cells to mature keratinocytes. Positive control for XOR was mouse liver.

compared with wounds from control mice (Figure 2C). Measurement of XOR activity showed that allopurinol applied to the wounds markedly reduced XOR activity by over 70% compared with control wound tissues (156.2 ± 90.5 μU/mg versus 547.4 ± 15.9, respectively; n = 3/group; $P = 0.013$).

Minimal Expression of Other Mb-Containing Oxidases Was Detected in Wound Tissue

AO and sulfite oxidase (SO) both contain Mb and can be inhibited by tungsten. They can also function as nitrite reductases. Very low levels of AO were detected in the skin and wound tissues by Western blot (Figure 2D). SO, which is primarily mitochondrial, was not detectible in the wounds as well (data not shown). Assay of wound tissues for AO activity showed no detectable oxidation of DMAC (n = 3), supporting the absence of AO activity in wounds. These findings support that the predominant effect of tungsten on wound healing is mediated through XOR.

XOR Inhibition with Tungsten Reduced ROS/RNS in Granulation Tissue

To determine the effect of dietary tungsten or allopurinol on wound levels of ROS/RNS, granulation tissue was collected at d 5. By using the OxiSelect In Vitro ROS/RNS Assay, granulation tissue from control mice had similar levels of ROS/RNS as wounds from mice treated with dietary allopurinol (Figure 3A). However, tungsten reduced wound ROS/RNS by ~60%, confirming the efficient inhibition of XOR by tungsten but not dietary allopurinol (n = 7/group; $P < 0.01$ versus control, $P < 0.05$ versus allopurinol). In a separate experiment, topical allopurinol did significantly reduce wound ROS/RNS production compared with untreated wounds (n = 3/group, 0.55 ± 0.10 versus 1.00 ± 0.09-fold change; $P = 0.029$).

XOR Inhibition with Tungsten Reduced Wound Angiogenesis and KC Proliferation

Tissue sections from healed wounds were stained for CD31 as a marker for ECs (Figure 3B). Wounds from tungsten-treated mice had 25.3% fewer CD31-positive luminal structures versus wounds from control mice (Figure 3C; $P < 0.05$; n = 6). Wound proliferation was measured by Ki67 staining at d 7. Ki67 was most prominent in the wound edge basilar KCs in control mice (30.7 ± 5.3%, Figure 3D). However, tungsten-treated mice (Figure 3D) had significantly fewer proliferating basilar KCs (9.1 ± 4.8%, $P < 0.05$).

Topical H_2O_2 Reversed Tungsten-Induced Delay in Wound Healing and Improved Angiogenesis

To determine if the role of XOR in wound healing was mediated through

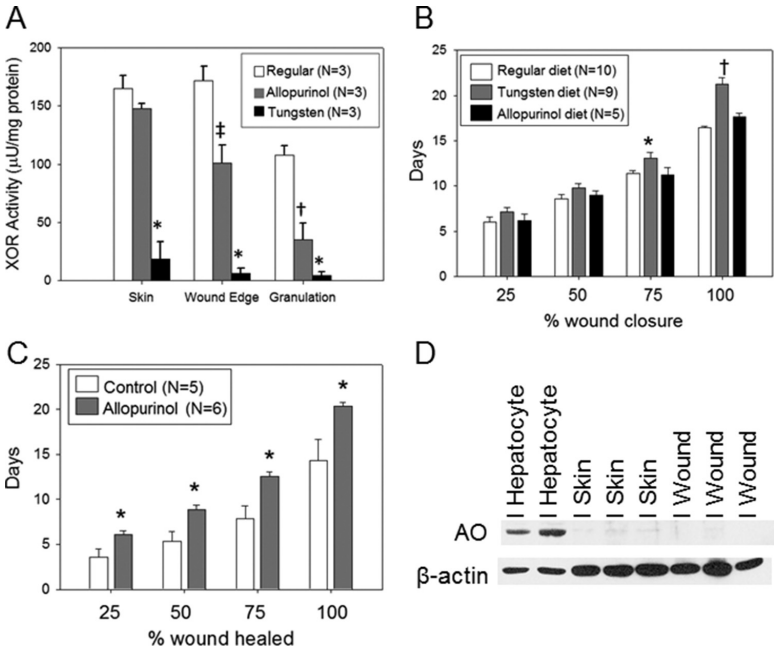

Figure 2. Effect of XOR inhibition on excisional wound-healing rates. (A) XOR activity was measured in the skin, wound edge and granulation tissue in control, tungsten-fed or allopurinol-fed mice (n = 3 mice/group; $^{*}P < 0.05$ versus control and allopurinol groups, $^{\ddagger}P < 0.05$ versus control and tungsten groups). (B) Wound healing rates in control, tungsten-fed and allopurinol-fed mice as reported as days to reach 25%, 50%, 75% and 100% wound closure ($^{*}P < 0.05$ and $^{\dagger}P < 0.001$ versus regular or allopurinol diet). (C) Effect of topical allopurinol on wound healing (n = 5–6 mice/group; $P < 0.05$ at all wound sizes). (E) Western blot for AO expression in the skin and wound tissue of control mice with hepatocytes serving as the positive control.

H_2O_2 production, wounds were treated topically with 0.15% H_2O_2 or saline every other day until complete wound closure. H_2O_2 did not alter wound healing rates in control mice (Figure 3E), but it significantly improved healing in tungsten-fed mice versus tungsten diet alone (18.5 ± 0.7 versus 21.0 ± 0.7 d; $P < 0.01$), approaching the rates in control mice. H_2O_2 treatment of wounds in tungsten-treated mice showed a trend toward improved angiogenesis (Figure 3F; $P = 0.067$).

Dietary Nitrite Manipulations Did Not Alter Systemic Levels of Nitrite or Wound Healing

Mice receiving supplemental sodium nitrite showed no improvement in wound healing compared with controls (17.4 ± 0.3 versus 16.7 ± 0.3 d, P = nonsignificant [NS], n = 5). Similarly, mice on a nitrite-free diet showed no change in wound healing versus controls (17.2 ± 0.3 versus 16.7 ± 0.3 d, respectively; P = NS). However, serum nitrite levels remained unchanged in mice receiving nitrite supplementation or depletion compared with regular chow (282.5 ± 35.5 versus 254.8 ± 64.0 versus 199.3 ± 53.9 nmol/L, respectively; $P = 0.54$, n = 4). The inability to change serum nitrite levels with diet may explain the lack of effect observed.

XOR Mediates KC and EC Function

KCs are the predominant cell type in the wounds expressing XOR and tungsten inhibition of XOR reduced basilar KC proliferation. Thus, we evaluated the effect of XOR activity on KCs *in vitro*. Inhibition of XOR with allopurinol did not affect proliferation in cultured human KCs (Figure 4A). Nitrite treatment significantly increased KC proliferation, which was reversed by allopurinol, indicating nitrite functioned through XOR to promote proliferation. H_2O_2 also increased KC proliferation.

Because tungsten also reduced wound angiogenesis, the role of XOR in EC function was also examined. By Western blot, cultured human ECs express XOR at baseline (data not shown). There was a trend toward reduced proliferation when ECs were treated with allopurinol (P = 0.064) and catalase ($P = 0.073$) (Figure 4B), suggesting XOR and H_2O_2 contribute to baseline EC proliferation. Nitrite significantly increased EC proliferation, and this was reversed with allopurinol, indicating that nitrite effects were mediated by XOR. Treatment with H_2O_2 also increased proliferation. Similarly, nitrite and H_2O_2 both increased cell migration (Figure 4C). Allopurinol did not alter migration but nitrite could enhance XOR-mediated NO production to increase migration, suggesting that XOR did not regulate baseline migration but could be used to improve migration with nitrite. EC tubing, a measure of angiogenic activity, was inhibited by allopurinol, which reduced box formation and reduced the number of long tubes (Figures 4D, E). Nitrite significantly increased tubing complexity and tube lengths in an allopurinol reversible fashion.

DISCUSSION

Our investigations identified a novel role for XOR in the normal wound healing process. High levels of XOR expression were detected in the skin and wound edge of normal mice, with most of the expression located within the basilar KCs. This expression was upregulated shortly after wounding and likely coincides with the proliferative activity of the KCs at the wound edge. This enhanced XOR expression is observed throughout the healing process and likely subsides as the KCs stop proliferating and the epidermis matures. We also observed XOR expression in the early inflammatory infiltrates in the wound. XOR inhibition with tungsten significantly delayed wound closure. Local wound inhibition of XOR with topical al-

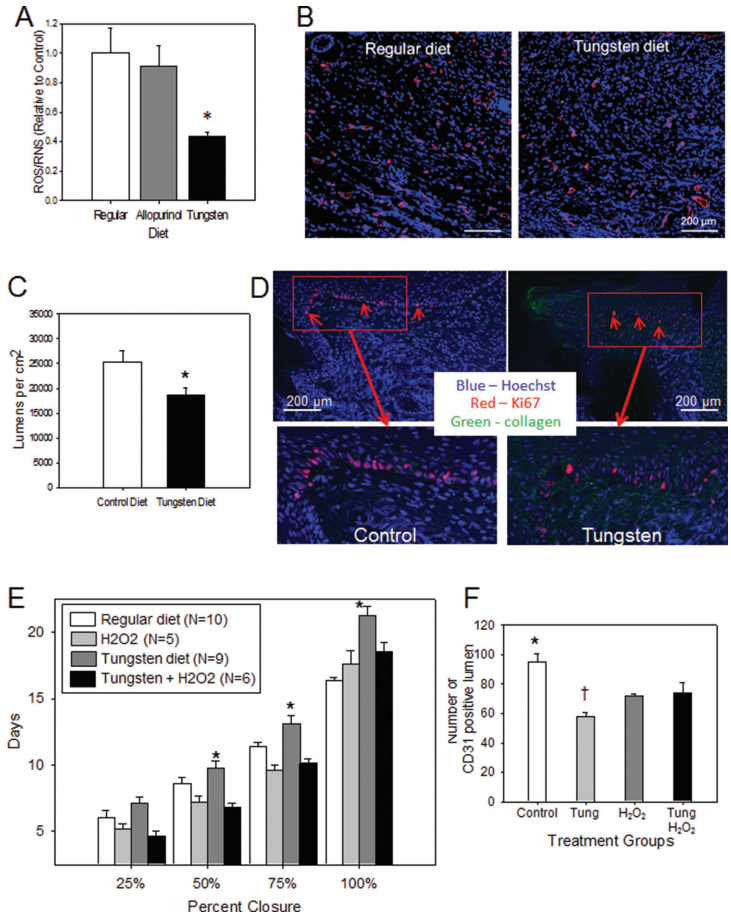

Figure 3. Effect of XOR inhibition on wound angiogenesis and proliferation. (A) Effect of tungsten and allopurinol diet on wound ROS/RNS production. Wound tissue was collected from mice at 5 d after wounding. ROS/RNS production was measured by using the OxiSelect In Vitro ROS/RNS Assay Kit, which detects H_2O_2, peroxyl radical, NO and peroxynitrite anion. Levels of ROS/RNS are normalized to the levels measured in mice fed regular diets (n = 5 mice/group, **P* = 0.006 versus regular diet and *P* = 0.016 versus allopurinol diet). (B) Effect of XOR inhibition on wound angiogenesis, as indicated by CD31-positive structures, was examined in wound tissues collected from control mice and tungsten fed mice immediately upon wound closure (CD31 for ECs, red; Hoechst 33325 for nuclei, blue; collagen, green). Representative photomicrographs of wounds from mice fed regular and tungsten diets are shown (100× magnification). (C) Quantification of wound angiogenesis was performed by counting luminal structures (two sections per wound, n = 6/group; **P* < 0.05 versus control diet). (D) Effect of XOR inhibition with tungsten on wound keratinocyte proliferation. Wound tissue was collected from control and tungsten diet–fed mice at d 7 after wounding. Tissues were stained for cell proliferation with Ki67 (red) and for cell nuclei with Hoechst 33325 (blue). Representative photomicrographs (100× magnification) are shown. Red arrows indicate proliferating basilar KCs at the wound edge. Magnified views of the red box areas are provided. (E) Effect of H_2O_2 on wound healing in tungsten-treated mice. C57BL/6 mice were fed either regular diet or a tungsten-enriched diet starting 2 wks before wounding and then maintained. Wounds were treated with either topical H_2O_2 (0.15%) or saline application every other day. Wounds were measured every other day until complete closure. The time required to achieve 25%, 50%, 75% and 100% closure for each treatment group is presented graphically (**P* < 0.01 versus H_2O_2 and tungsten + H_2O_2). (F) Quantification of wound angiogenesis was performed in wounds treated with and without H_2O_2. Data are presented as number of CD31-positive lumen structures per high-power field (n = 6/treatment; **P* < 0.02 versus all other groups; †*P* = 0.067 versus tungsten + H_2O_2).

lopurinol also significantly delayed wound healing. Both of these findings support an important role for XOR in wound repair. The ability to reverse effect of tungsten with topical H_2O_2 suggests that XOR contributes to wound H_2O_2 production and is required for normal healing. *In vitro* studies demonstrated the ability of XOR to mediate pro-angiogenic functions in ECs and proliferation in KCs. These findings together strongly support the contribution of XOR in the normal wound healing process.

XOR represents a mix of xanthine oxidase (XO) and dehydrogenase (XDH) (both are involved in purine metabolism [21]) and is clinically notable for its role in gout, where metabolism of xanthine to uric acid (UA) results in joint deposition and inflammation. This pathway also yields H_2O_2 and superoxide, both of which are associated with tissue injury during ischemia/reperfusion (I/R) (33,34). Inhibition of XOR reduces ROS-mediated I/R injury (28). In the setting of ischemia and hypoxia, XO predominates and more efficiently generates superoxide, although XDH also possesses partial oxidase activity (35). While detrimental in excess, physiologic levels of ROS are essential in cell signaling (36) and tissue homeostasis and repair (6,7). Most tissue production of ROS has been attributed to nicotinamide adenine dinucleotide phosphate (NADPH) oxidase, and the role of XOR in the generation of physiologic ROS has been underappreciated. More recently, XOR gained attention for its ability to convert nitrite to NO to mediate cytoprotection (23,37). We and others have shown that XOR is required for the beneficial actions of supplemental nitrite in the inhibition of intimal hyperplasia after vascular injury (23) and in reversing pulmonary hypertension (24). XOR expression in skin has been previously reported, linked to the pathogenesis of sunburn and skin inflammation (24,25). Beyond that, little is known about the role of XOR in the skin.

XOR inhibition with dietary tungsten significantly delayed wound closure. Tungsten replaces the Mb within XOR,

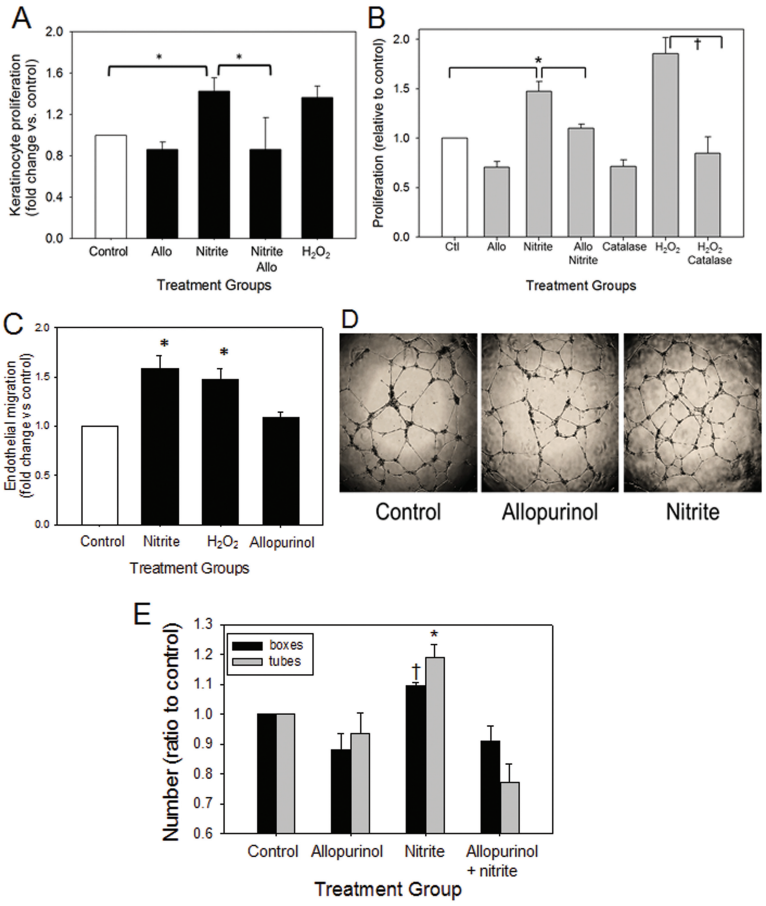

Figure 4. Effect of XOR function on keratinocyte and endothelial cell behavior *in vitro*. (A) Human KCs were cultured in 1% serum media with allopurinol (allo; 100 μmol/L), nitrite (100 μmol/L), nitrite + allopurinol and H_2O_2 (250 μmol/L) for 24 h. Proliferation was measured by ^{3}H-thymidine uptake, and results are expressed as fold-change over control (mean ± SEM of four experiments; $^*P < 0.05$ nitrite versus control or nitrite + allopurinol). (B) ECs were grown in 1% serum media with the addition of allopurinol (allo; 100 μmol/L), nitrite (100 μmol/L), nitrite + allopurinol, H_2O_2 (250 μmol/L), catalase (1,000 U) or catalase + H_2O_2. EC proliferation was quantified by ^{3}H-thymidine incorporation at 24 h (mean ± SEM of 6–11 experiments; $^*P < 0.05$ versus control and nitrite + allopurinol; $^\dagger P < 0.001$ versus H_2O_2 + catalase). (C) EC migration was measured using the scratch assay. Cells were treated with nitrite (100 μmol/L), H_2O_2 (125 μmol/L) or allopurinol (100 μmol/L), and migration was quantified at 24 h by measuring the area occupied by cells within the scratch and normalizing to that achieved by control ECs (mean ± SEM of three separate experiments; $^*P < 0.01$ versus control and allopurinol). (D) EC capillary tubing was performed by culturing the ECs on Matrigel™ with allopurinol or nitrite. Photomicrographs are shown from 6 h (representative of six experiments). (E) Quantification of EC tubing was performed by counting box formation and total number of tubes measuring >110 pixels in length as an indicator of long tubes (mean ± SEM of six separate experiments; long tube number $^*P < 0.05$ versus all other groups; box number $^\dagger P = 0.011$ versus allopurinol + nitrite).

irreversibly inhibiting its function (21). However, Mb is also essential for other oxidoreductases such as AO and SO. We found low levels of these enzymes in wound tissues. The other inhibitor of XOR that we used was allopurinol, a drug used to clinically treat gout and as an investigative tool in other experiments (23,24). In our studies, dietary allopurinol did not alter wound healing rates and raised concerns that tungsten effects may be mediated by actions on AO or SO. However, we identified essentially no AO or SO expression and no measurable AO activity as well in untreated wounds. We did find that tungsten dramatically inhibited skin and wound XOR activity, while dietary allopurinol only reduced it modestly in the wound edge and granulation tissue. Allopurinol has been used to block XOR activity in other tissues, such as in carotid and pulmonary arteries, but was much less effective in our model. The reduced ability of allopurinol to inhibit XOR in wounds may be due to poor biodistribution in the relatively hypoperfused wound bed and skin. Its bioavailability may also be diminished by renal clearance and the requirement for conversion to its active form, oxypurinol (38,39). In addition, the binding of XOR to endothelial glycosaminoglycans results in resistance to allopurinol (38,39). In contrast, topical allopurinol significantly delayed wound closure and reduced XOR activity and wound ROS/RNS levels. These findings confirm the role of wound XOR function in mediating normal wound repair. They also illustrate the potential ability to target wound XOR by topical treatments.

NO is required for normal tissue repair (12,14), and its deficiency contributes to delayed wound healing, whereas NOS gene transfer restores healing rates to normal (19). Diabetic wounds have reduced NOS expression and NO production (16,18), resulting in delayed wound healing. Arginase I is also upregulated during wound healing (16) for the production of polyamines that are essential for cell proliferation and collagen synthesis but competes with NOS for arginine and can reduce NO production (17). Dietary nitrite can serve as an alternate source of NO through XOR (21,22). This pathway has been shown to be biologically important in the setting of vascular injury and pulmonary hypertension where dietary nitrite reduced the adverse

vascular remodeling (23,24,37). On the basis of these reports and the abundance of XOR in skin, we proposed that wound NO production may be increased through XOR-mediated nitrite conversion to NO. Harnessing this local nitrite reductase activity may be an attractive mechanism to increase wound NO production in settings where NOS activity is reduced, such as diabetic wounds (15–18). In our study, neither dietary nitrite depletion nor supplementation altered healing rates. Measurements of serum nitrite levels revealed that these dietary manipulations did not change serum nitrite levels. A potential explanation for these findings is that systemic nitrite production may contribute to significant serum stores, making it difficult to reduce or elevate systemic levels with diet alone. The poor vascularity of the wounds may also reduce tissue nitrite bioavailability. Thus, no conclusion can yet be drawn about the ability to manipulate XOR-mediated NO production in wound healing. In addition, normal wound healing is efficient and difficult to improve. Future studies will examine XOR in models of impaired wound healing such as diabetes.

Other products of XOR that may contribute to wound healing are ROS. While high levels of ROS in the skin are linked to injury and disease (40,41), physiologic levels of ROS, particularly H_2O_2, are essential for wound repair (6,8). Overexpression of catalase, which breaks down H_2O_2, delayed wound healing, whereas physiologic levels of H_2O_2 applied to a wound-enhanced healing (6). In zebrafish, H_2O_2 production is upregulated immediately after wounding and promotes the inflammatory phase by rapid leukocyte recruitment (8). The decomposition of H_2O_2 stalled vascular endothelial growth factor (VEGF)–VEGF receptor signaling and impaired angiogenesis and wound healing (42). In all of these studies, NADPH oxidase was determined to be the source of the H_2O_2 and other ROS. In the tungsten-fed mice and in topical allopurinol-treated wounds, ROS/RNS levels were significantly reduced, suggesting that a deficiency in oxidants contributes to poor wound healing. In a hypoxic environment, such as the wound bed, the predominant ROS generated by XOR is H_2O_2 (43). Thus, we applied dilute H_2O_2 topically on wounds in tungsten-fed mice and restored healing to near normal and improved wound angiogenesis. These findings support that XOR production of ROS/RNS, likely H_2O_2, mediates normal wound healing that was previously attributed to NADPH oxidase. Our studies do not quantify or discount the role of NADPH oxidase–derived ROS/H_2O_2 in wound healing but strongly support the important contribution of XOR in the production of oxidants necessary for normal biologic processes. Interestingly, Nam *et al.* (44) showed that NADPH oxidase inhibition reduced KC H_2O_2 production at early time points (30 min) but did not alter production at 20 h, supporting an alternate source of H_2O_2.

Another product of XOR function is UA. UA has been associated with inflammation and has been detected in wound fluids, where its concentrations correlated with degree of impaired healing (45). UA may have direct injurious actions independent of XOR-derived ROS, but this has yet to be determined. We hypothesize that, in the setting of abnormal wound repair, such as in diabetes, XOR may be upregulated and leads to the increased oxidative stress that results in protracted inflammation and poor healing. NO and H_2O_2 have been implicated in KC proliferation and in the modulation of epidermal growth factor receptor in lung and human foreskin KC (46,47). Similarly, they have also been implicated in wound angiogenesis (5). We found prominent proliferation in the basilar KC lining the wound edge, and tungsten reduced the number of proliferating KCs in the wound. We also observed reduced angiogenesis in wounds from tungsten-treated mice, supporting a role for XOR in wound angiogenesis. Our *in vitro* studies confirm an important role for XOR in mediating EC proliferation, migration and angiogenic activity. Allopurinol blocked proliferation and tube formation *in vitro*, indicating that endogenous XOR activity contributes to these key EC behaviors. The ability of nitrite and H_2O_2 to enhance EC proliferation and migration suggests that both NO and H_2O_2 production likely mediate the wound-healing properties of XOR *in vivo*. Kou *et al.* (48) reported the role of endogenous XO in maintaining VEGF-induced EC survival. It was also reported that NO derived from XOR regulates hypoxia-inducible factor 1-α (HIF1α)- and VEGF-dependent angiogenesis (49). The impaired angiogenesis resulting from XOR inhibition may be due to loss of H_2O_2-mediated induction of angiogenic VEGF (42). It was also shown that VEGF downstream signaling depends on ROS production (42), again presumably through NADPH oxidase. Future studies will isolate the contribution of XOR-derived ROS from that of NADPH oxidase.

Isolated XOR deficiency in humans is rare and is only documented in a few case reports (50,51). However, Mb cofactor deficiency has been described and is associated with severe refractory seizure activity with childhood fatality (reviewed in ref. [52]). Global XOR deficiency is fatal, and, thus, no XOR-deficient mouse is currently available to assist in the investigation of XOR function in wound healing. The generation of tissue-specific or conditional XOR knockouts will be extremely helpful and is currently underway.

CONCLUSION

We provide the first evidence that XOR contributes to normal wound healing. Our data showed that XOR stimulates KC proliferation and wound angiogenesis through the production of ROS. The *in vitro* effects of XOR on EC behavior are mediated by both NO and H_2O_2. Future studies are necessary to better define the role of XOR-mediated NO generation in these effects. In addition, it is important to determine how XOR activity is regulated in impaired wound healing such as in diabetes, venous stasis and ischemia. Targeting wound XOR may provide a way to manipulate local ROS and

NO production, possibly achieved through topical routes that are extremely attractive in the management of patients with difficult wounds.

ACKNOWLEDGMENTS

We gratefully acknowledge the excellent technical assistance provided by NJ Hundley, SI Zharikov and N Cantu-Medellin. This material is based on work supported in part by the Department of Veterans Affairs, Veterans Health Administration and Office of Biomedical Laboratory Research and Development (ET), through funding from the National Institutes of Health (NIH) (NIH T32 HL098036 to MC Madigan, RM McEnaney and AJ Shukla and NIH R01 HL058115 to MM Tarpey). M Gladwin received research support from NIH grants R01HL098032, R01HL096973 and PO1HL103455 as well as from the Institute for Transfusion Medicine and the Hemophilia Center of Western Pennsylvania.

The contents of this manuscript do not represent the views of the Department of Veterans Affairs or the United States Government.

DISCLOSURE

The authors declare that they have no competing interests as defined by *Molecular Medicine*, or other interests that might be perceived to influence the results and discussion reported in this paper.

REFERENCES

1. Singh N, Armstrong DG, Lipsky BA. (2005) Preventing foot ulcers in patients with diabetes. *JAMA*. 293:217–28.
2. Barrientos S, Stojadinovic O, Golinko MS, Brem H, Tomic-Canic M. (2008) Growth factors and cytokines in wound healing. *Wound Repair Regen.* 16:585–601.
3. Smiell JM, *et al.* (1999) Efficacy and safety of becaplermin (recombinant human platelet-derived growth factor-BB) in patients with non-healing, lower extremity diabetic ulcers: a combined analysis of four randomized studies. *Wound Repair Regen*. 7:335–46.
4. Soneja A, Drews M, Malinski T. (2005) Role of nitric oxide, nitroxidative and oxidative stress in wound healing. *Pharmacol. Rep.* 57 Suppl:108–19.
5. Schafer M, Werner S. (2008) Oxidative stress in normal and impaired wound repair. *Pharmacol. Res.* 58:165–71.
6. Roy S, Khanna S, Nallu K, Hunt TK, Sen CK. (2006) Dermal wound healing is subject to redox control. *Mol. Ther.* 13:211–20.
7. Sen CK, Roy S. (2008) Redox signals in wound healing. *Biochim. Biophys. Acta.* 1780:1348–61.
8. Niethammer P, Grabher C, Look AT, Mitchison TJ. (2009) A tissue-scale gradient of hydrogen peroxide mediates rapid wound detection in zebrafish. *Nature*. 459:996–9.
9. Senel O, Cetinkale O, Ozbay G, Ahcioglu F, Bulan R. (1997) Oxygen free radicals impair wound healing in ischemic rat skin. *Ann. Plast. Surg.* 39:516–23.
10. Loo AE, *et al.* (2012) Effects of hydrogen peroxide on wound healing in mice in relation to oxidative damage. *PLoS One.* 7:e49215.
11. Lee RH, Efron D, Tantry U, Barbul A. (2001) Nitric oxide in the healing wound: a time-course study. *J. Surg. Res.* 1001:104–8.
12. Fukumura D, *et al.* (2001) Predominant role of endothelial nitric oxide synthase in vascular endothelial growth factor-induced angiogenesis and vascular permeability. *Proc. Natl. Acad. Sci. U. S. A.* 98:2604–9.
13. Schäffer MR, *et al.* (1997) Nitric oxide, and autocrine regulator of wound fibroblast synthetic function. *J. Immunol.* 158:2375–81.
14. Ziche M, *et al.* (1994) Nitric oxide mediates angiogenesis in vivo and endothelial cell growth and migration in vitro promoted by Substance P. *J. Clin. Invest.* 94:2036–44.
15. Schäffer MR, *et al.* (1997) Diabetes-impaired healing and reduced wound nitric oxide synthesis: a possible pathophysiologic correlation. *Surgery.* 121:513–9.
16. Kampfer H, Pfeilschifter J, Frank S. (2003) Expression and activity of arginase isoenzymes during normal and diabetes-impaired skin repair. *J. Invest. Dermatol.* 121:1544–51.
17. Albina JE, Mills CD, Henry WL, Caldwell MD. (1990) Temporal expression of different pathways of L-arginine metabolism in healing wounds. *J. Immunol.* 144:3877–80.
18. Stallmeyer B, *et al.* (2002) Regulation of eNOS in normal and diabetes-impaired skin repair: implications for tissue regeneration. *Nitric Oxide.* 6:168–77.
19. Yamasaki K, *et al.* (1998) Reversal of impaired wound repair in iNOS-deficient mice by topical adenoviral-mediated iNOS gene transfer. *J. Clin. Invest.* 101:967–71.
20. Lee PC, *et al.* (1999) Impaired wound healing and angiogenesis in eNOS-deficient mice. *Am. J. Physiol.* 277:H1600–8.
21. Brondino CD, Romao MJ, Moura I, Moura JJ. (2006) Molybdenum and tungsten enzymes: the xanthine oxidase family. *Curr. Opin. Chem. Biol.* 10:109–14.
22. Li H, Cui H, Kundu TK, Alzawahra W, Zweier JL. (2008) Nitric oxide production from nitrite occurs primarily in tissues not in the blood. *J. Biol. Chem.* 283:17855–63.
23. Alef MJ, *et al.* (2011) Nitrite-generated NO circumvents dysregulated arginine/NOS signaling to protect against intimal hyperplasia in Sprague-Dawley rats. *J. Clin. Invest.* 121:1646–56.
24. Zuckerbraun BS, *et al.* (2010) Nitrite potently inhibits hypoxic and inflammatory artery hypertension and smooth muscle proliferation via xanthine oxidoreductase-dependent nitric oxide generation. *Circulation*. 121:98–109.
25. Nakai K, Kadiiska MB, Jiang JJ, Stadler K, Mason RP. (2006) Free radical production requires both inducible nitric oxide synthase and xanthine oxidase in LPS-treated skin. *Proc. Natl. Acad. Sci. U. S. A.* 103:4616–21.
26. Portugal-Cohen M, *et al.* (2011) Skin organ culture as a model to study oxidative stress, inflammation and structural alterations associated with UVB-induced photodamage. *Exp. Dermatol.* 20:749–55.
27. Johnson JL, Rajagopalan KV, Cohen HJ. (1974) Molecular basis of the biological function of molybdenum. *J. Biol. Chem.* 249:859–66.
28. Pacher P, Nivorozhkin A, Szabo A. (2006) Therapeutic effects of xanthine oxidase inhibitors: renaissance half a century after the discovery of allopurinol. *Pharmacol. Rev.* 58:87–114.
29. Committee for the Update of the Guide for the Care and Use of Laboratory Animals, Institute for Laboratory Animal Research, Division on Earth and Life Studies, National Research Council of the National Academies. (2011) *Guide for the Care and Use of Laboratory Animals*. 8th edition. Washington (DC): National Academies Press.
30. Sachdev U, *et al.* (2012) High mobility group box 1 promotes endothelial cell angiogenic behavior in vitro and improves muscle perfusion in vivo in response to ischemic injury. *J. Vasc. Surg.* 55:180–91.
31. Kibbe MR, *et al.* (2000) Inducible nitric oxide synthase (iNOS) expression upregulates p21 and inhibits vascular smooth muscle cell proliferation through p42/44 mitogen-activated protein kinase activation and independent of p53 and cyclic guanosine monophosphate. *J. Vasc. Surg.* 31:1214–28.
32. Liang CC, Park AY, Guan JL. (2007) In vitro scratch assay: a convenient and inexpensive method for analysis of cell migration in vitro. *Nat. Protoc.* 2:329–33.
33. Adkins WK, Taylor AE. (1990) Role of xanthine oxidase and neutrophils in ischemia-reperfusion injury in rabbit lung. *J. Appl. Physiol.* 69:2012–8.
34. White CR, *et al.* (1996) Circulating plasma xanthine oxidase contributes to vascular dysfunction in hypercholesterolemic rabbits. *Proc. Natl. Acad. Sci. U. S. A.* 93:8745–9.
35. Linas SL, Whittenburg D, Repine JE. (1990) Role of xanthine oxidase is ischemia/reprofusion injury. *Am. J. Physiol.* 258:F711–6.
36. Sen CK. (2003) The general case for redox control and wound repair. *Wound Repair Regen.* 11:431–8.
37. Baliga RS, *et al.* (2012) Dietary nitrate ameliorates pulmonary hypertension: cytoprotective role for

endothelial nitric oxide synthase and xanthine oxidoreductase. *Circulation*. 125:2922–32.
38. Malik UZ, *et al.* (2011) Febuxostat inhibition of endothelial-bound XO: implications for targeting vascular ROS production. *Free Radic. Biol. Med.* 51:179–84.
39. Kelley EE, *et al.* (2004) Binding of xanthine oxidase to glycosaminoglycans limits inhibition by oxypurinol. *J. Biol. Chem.* 279:37231–4.
40. Pence BC, Reiners JJ Jr. (1987) Murine epidermal xanthine oxidase activity: correlation with degree of hyperplasia induced by tumor promoters. *Cancer Res.* 47:6388–92.
41. Vermeij WP, Backendorf C. (2010) Skin cornification proteins provide global link between ROS detoxification and cell migration during wound healing. *PLoS One.* 5:e11957.
42. Roy S, Khanna S, Sen CK. (2008) Redox regulation of the VEGF signaling path and tissue vascularization: hydrogen peroxide, the common link between physical exercise and cutaneous wound healing. *Free Radic. Biol. Med.* 44:180–92.
43. Kelley EE, *et al.* (2010) Hydrogen peroxide is the major oxidant product of xanthine oxidase. *Free Radic. Biol. Med.* 48:493–8.
44. Nam HJ, Park YY, Yoon G, Cho H, Lee JH. (2010) Co-treatment with hepatocyte growth factor and TGF-β1 enhance migration of HaCaT cells through NADPH oxidase-dependent ROS generation. *Exp. Mol. Med.* 42:270–9.
45. Fernandez ML, Upton Z, Shooter GK. (2014) Uric acid and xanthine oxidoreductase in wound healing. *Curr. Rheumatol. Rep.* 16:396.
46. Goldkorn T, *et al.* (1998) EGF-receptor phosphorylation and signaling are targeted by H2O2 redox stress. *Am. J. Respir. Cell Mol. Biol.* 19:786–98.
47. Peus D, *et al.* (1998) H_2O_2 is an important mediator of UVB-induced EGF-receptor phosphorylation in cultured keratinocytes. *J. Invest. Dermatol.* 110:966–71.
48. Kou B, Ni J, Vatish M, Singer DR. (2008) Xanthine oxidase interaction with vascular endothelial growth factor in human endothelial cell angiogenesis. *Microcirculation.* 15:251–67.
49. Bir SC, *et al.* (2012) Hydrogen sulfide stimulates ischemic vascular remodeling through nitric oxide synthase and nitrite reduction activity regulating hypoxia-inducible factor-1a and vascular endothelial growth factor-dependent angiogenesis. *J. Am. Heart Assoc.* 1:e004093.
50. Ichida, K, *et al.* (1997) Identification of two mutations in human xanthine dehydrogenase gene responsible for classical type I xanthinuria. *J. Clin. Invest.* 99:2391–7.
51. Mateos FA, Puig JG, Jimenez ML, Fox IH. (1987) Hereditary xanthinuria: evidence for enhanced hypozanthine salvage. *J. Clin. Invest.* 79:847–52.
52. Reiss J, Johnson JL. (2003) Mutations in the molybdenum cofactor biosynthetic genes MOCS1, MOCS2, and GEPH. *Hum. Mutat.* 21:569–76.

Cite this article as: Madigan MC, *et al*. (2015) Xanthine oxidoreductase function contributes to normal wound healing. *Mol. Med*. 21:313–22.